AGU ADVANCING EARTH AND SPACE SCIENCE

Geophysical Research Letters

RESEARCH LETTER
10.1029/2021GL093722

Key Points:

- Circulation patterns inducing wintertime $PM_{2.5}$ pollution in Delhi are identified using self-organizing map classification
- Climate models project decrease (increase) in frequency of pollution (clean)-favorable circulation pattern throughout the 21st century
- Warming trends of sea surface temperature in the central Pacific and Atlantic Oceans lead to decrease in pollution-favorable circulation

Supporting Information:

Supporting Information may be found in the online version of this article.

Correspondence to:

H. Liao,
hongliao@nuist.edu.cn

Citation:

Li, J., Hao, X., Liao, H., Hu, J., & Chen, H. (2021). Meteorological impact on winter $PM_{2.5}$ pollution in Delhi: Present and future projection under a warming climate. *Geophysical Research Letters*, *48*, e2021GL093722. https://doi.org/10.1029/2021GL093722

Received 8 APR 2021
Accepted 22 JUN 2021

Meteorological Impact on Winter $PM_{2.5}$ Pollution in Delhi: Present and Future Projection Under a Warming Climate

Jiandong Li[1], Xin Hao[2,3], Hong Liao[1], Jianlin Hu[1], and Haishan Chen[4]

[1]Jiangsu Key Laboratory of Atmospheric Environment Monitoring and Pollution Control, Jiangsu Collaborative Innovation Center of Atmospheric Environment and Equipment Technology, School of Environmental Science and Engineering, Nanjing University of Information Science & Technology, Nanjing, China, [2]Collaborative Innovation Center on Forecast and Evaluation of Meteorological Disasters/Key Laboratory of Meteorological Disaster, Ministry of Education, Nanjing University for Information Science & Technology, Nanjing, China, [3]Nansen-Zhu International Research Centre, Institute of Atmospheric Physics, Chinese Academy of Sciences, Beijing, China, [4]Key Laboratory of Meteorological Disaster, Ministry of Education (KLME)/Joint International Research Laboratory of Climate and Environment Change (ILCEC)/Collaborative Innovation Center on Forecast and Evaluation of Meteorological Disasters (CIC–FEMD), Nanjing University of Information Science and Technology (NUIST), Nanjing, China

Abstract This study employs the self-organizing map classification to track wintertime $PM_{2.5}$ pollutions in Delhi under four atmospheric circulation patterns during 2013–2020. We found that the most polluted circulation pattern was characterized by a northward shift in the subtropical jet stream and a northward intrusion of the subtropical high, leading to descending anomalies from the upper troposphere to the near surface. Together, the resultant reduced passage of cyclones, lower planetary boundary layer, weakened near-surface winds and less precipitation contributed to wintertime $PM_{2.5}$ pollution in Delhi. Compared with the 1981–2010 mean levels, Coupled Model Intercomparison Project 6 models project Delhi would experience two fewer days of severe pollution-favorable circulation pattern and seven more days of clean-favorable circulation pattern in 2070–2099 under the shared socioeconomic pathway 5–8.5. Future decrease in the severe pollution-favorable circulation pattern may be attributed to the warming trends in sea surface temperature over the central Pacific and North Atlantic Ocean.

Plain Language Summary Delhi, the capital city of India, currently suffers severe fine particulate matter ($PM_{2.5}$) pollution, which poses serious public health hazards. The root cause of this problem is excessive emissions from power plants, vehicles, manufactures, and domestic heating released into the atmosphere. During winter, severe air pollutions with high $PM_{2.5}$ concentrations frequently occurred when coincided with bad weather conditions. Here, we show these unfavorable weather conditions were associated with a circulation pattern which can be captured by climate models. Global warming is projected to be a beneficial role throughout the whole 21st century, leading to decrease in pollution-favorable weather days and increase in clean-favorable weather days. Our findings have important implications for future air quality management in Delhi.

1. Introduction

Fine particulate matter ($PM_{2.5}$) is a major environmental concern for India. Approximately 50% of the population of India is exposed to $PM_{2.5}$ exceeding the Indian air quality standard of 40 μg m^{-3} (Chowdhury & Dey, 2016), and the resultant premature deaths attributable to long-term exposure to ambient $PM_{2.5}$ exceed 1 million (Cohen et al., 2017). The air pollution in India has a long history and is probably worsening because satellite-derived $PM_{2.5}$ shows a larger increase over 2010–2019 compared with 2000–2010 (Dey et al., 2020). Understanding the mechanism of particulate pollution in India is urgent for future air quality management.

Emissions, which mainly originate from residential biomass combustion, power plants and industrial coal combustion (Venkataraman et al., 2018), are the root cause of air pollution in India. The Indo-Gangetic Plain (IGP) in Northern India is an extremely densely populated area and experiences the highest $PM_{2.5}$ levels (Schnell et al., 2018). Emissions from the IGP contributed ~46% of total premature mortality over India (David et al., 2019). Among various emission sectors, household emissions are reported to be the largest contributor to $PM_{2.5}$ in India (Chowdhury et al., 2019). Complete mitigation of household emissions, including biomass for cooking, domestic heating and kerosene for lighting, would lead to a 30.7% improvement in the annual $PM_{2.5}$ concentration (Chowdhury et al., 2019).

In addition to high emissions, meteorology is generally considered to be an external factor driving day-to-day $PM_{2.5}$ variabilities. Numerous studies have investigated the correlation between local meteorological parameters and daily $PM_{2.5}$ concentrations. Meteorological conditions, including low wind speeds, shallow boundary layer heights and high relative humidity during winter in the IGP, favor pollution buildup (Nair et al., 2007; Ojha et al., 2020; Schnell et al., 2018), but the associated circulation characteristics and underlying process were not explored. Despite the lack of knowledge regarding the meteorological mechanisms modulating $PM_{2.5}$ pollution, pollution-favorable meteorological indices consisting of correlated meteorological parameters are used to project future meteorological conditions under a warming climate, but whether India would experience more (Horton et al., 2014) or less (Wu et al., 2019) polluted days remains controversial. In addition, the extreme topography of northern India adds complexity to this problem because near-surface meteorological conditions are reportedly decoupled from upper atmospheric circulations (Schnell et al., 2018). The lack of understanding of the impact of weather conditions on $PM_{2.5}$ pollution may increase the difficulty in future pollution-favorable meteorology predictions under global warming. In this study, we focused on winter particulate pollution in Delhi, which ranks as the most polluted city, and winter is the most polluted season (Singh et al., 2020). We aim to (a) understand the influence of circulation patterns on $PM_{2.5}$ pollution in Delhi, which has not been previously studied, and (b) project their future changes based on state-of-the-art climate models participating in Phase 6 of the Coupled Model Intercomparison Project (CMIP6) under a future warming scenario.

2. Data and Method

2.1. $PM_{2.5}$ Observations and Meteorological Data

We utilized an eight-year observed time series of $PM_{2.5}$ from the US embassy in New Delhi (77.186°E, 28.598°N, Figure 1b), available from the websites https://in.usembassy.gov/embassy-consulates/new-delhi/air-quality-data/ and https://www.airnow.gov/international/us-embassies-and-consulates/#India$New_Delhi, last access, May 22, 2021. This data set has been widely used in numerous previous studies (Chen et al., 2020; Gunthe et al., 2021; Singh et al., 2020; Sreekanth et al., 2018; Wu et al., 2019), and we found it could well represent $PM_{2.5}$ variations in Delhi (Text S1 and Figure S1). The quality control and daily averaged $PM_{2.5}$ are processed following a previous study (Li et al., 2019).

The meteorological fields used in this study are from ERA5 reanalysis data sets (Hersbach et al., 2020), with a spatial resolution of 2.5° × 2.5°. The pressure level variables with 37 pressure levels from the surface to 10 hPa from January 1979 to February 2020 include geopotential height, zonal and meridional winds, temperature, and relative humidity. The surface-level variables for the same period include sea level pressure (SLP) and zonal and meridional winds at 10 m. The observed sea surface temperatures (SSTs) from the Hadley Centre are downloaded from https://www.metoffice.gov.uk/hadobs/hadisst/data/download.html (Rayner et al., 2003).

Aerosol optical depth (AOD) from Moderate Resolution Imaging Spectroradiometer (MODIS) aerosol products is also used to present pollution distributions under each circulation type. The AOD data at the 550 nm wavelength in the MODIS daily global Level 3 products from 2013 to 2020 are obtained from https://ladsweb.modaps.eosdis.nasa.gov/search/, last access: May 22, 2021.

The daily global precipitation data (website: https://psl.noaa.gov/data/gridded/data.cpc.globalprecip.html, last access: May 22, 2021) are obtained to help understand weather condition effects on $PM_{2.5}$ pollution under each circulation type.

2.2. Circulation Pattern Classification

We employed the SOM (self-organizing map) method (Kohonen et al., 2001) in Cost733 software (https://projects.met.no/cost733/, last access: May 22, 2021) to classify typical wintertime circulation patterns in Delhi, and more details for SOM algorithm is provided in Text S2. This method has been widely applied

10.1029/2021GL093722

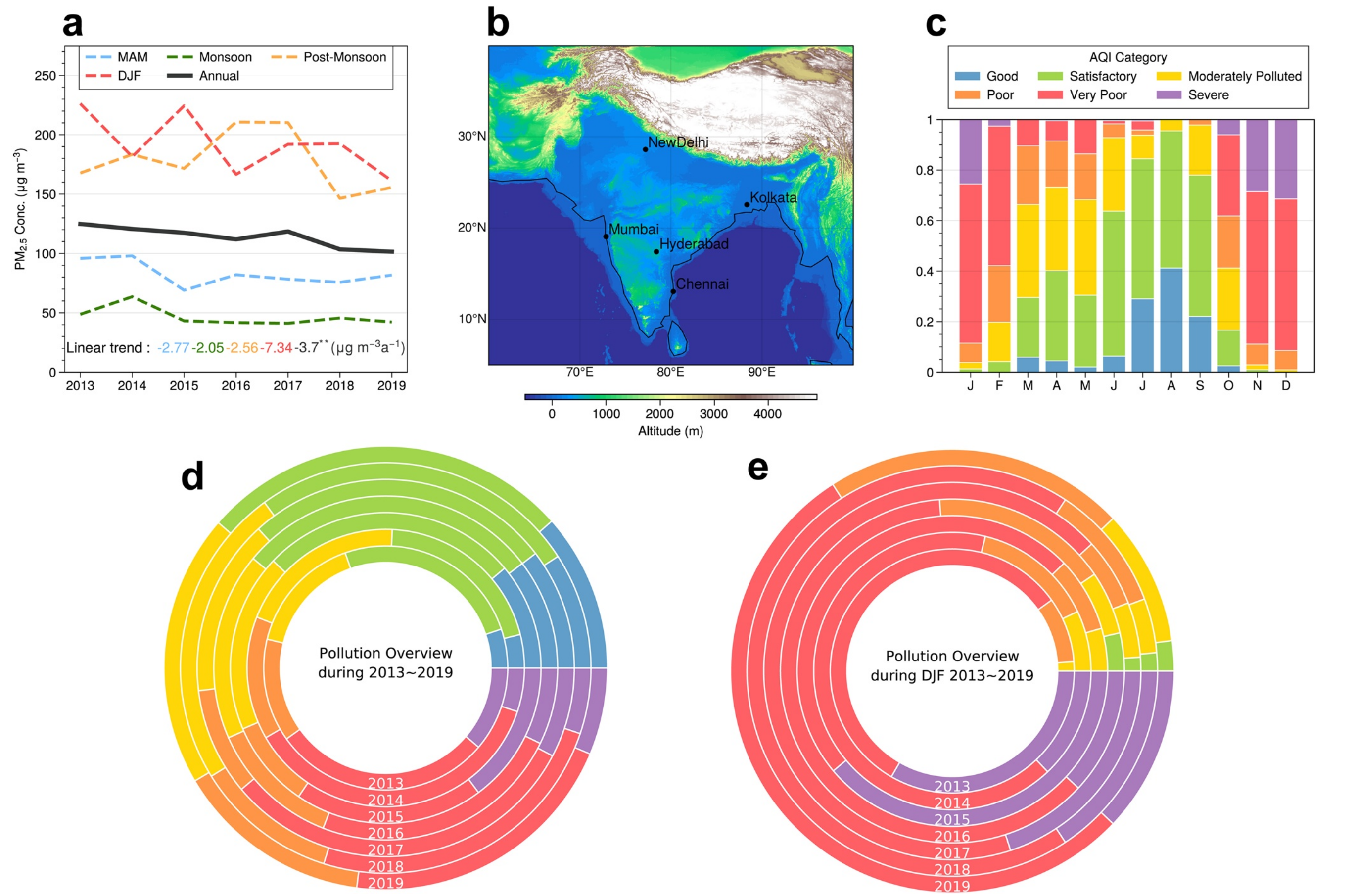

Figure 1. $PM_{2.5}$ pollution overview of Delhi from 2013 to 2019. (a) Time series of annual $PM_{2.5}$ concentrations in Delhi from 2013 to 2019. (b) Topographic map of India and locations of five US embassy locations with $PM_{2.5}$ observations. (c) Histogram of air quality index category frequencies for each month. (d–e) Frequency of pollution levels during 2013–2020 for the whole period (d) and December-January-February (e). (c–e) share the same legend in (c). $PM_{2.5}$ ranges for each level are Good: 0–30 μg m^{-3}, Satisfactory: 30–60 μg m^{-3}, Moderate: 60–90 μg m^{-3}, Poor: 90–120 μg m^{-3}, Very Poor: 120–250 μg m^{-3}, and Severe: >250 μg m^{-3}.

to study extreme events, such as heat waves (Horton et al., 2015), droughts (Zhuang et al., 2020), and air pollution (Callahan & Mankin, 2020; Liao et al., 2018).

To identify typical circulation patterns associated with $PM_{2.5}$ pollution, we utilize a correlation analysis to select optimal meteorological variables driving the daily variations in $PM_{2.5}$ concentrations. High correlations are found for zonal winds at 250 hPa (U250), meridional winds at 500 hPa, SLP, zonal winds at 10 m and meridional winds at 10 m (Figure S2). We choose U250 because (a) the major weather system influencing northern India during winter is the Western Disturbance (WD), a subtropical cyclone embedded in the subtropical jet stream (Dimri et al., 2016; Hunt et al., 2018), which can be revealed by U250. (b) U250 has high correlations with $PM_{2.5}$, and can well distinguish among each circulation type. The study region for classification is determined by a correlation map (Figure S2) between U250 and $PM_{2.5}$ (30°–80°E, 0°–40°N). We perform SOM classification on the winter (DJF, December-January-February) U250 fields over 1979–2019.

2.3. CMIP6 Model Output

We use the U250 from models participating in the CMIP6 to obtain future projections. There are 30 models for which daily U250 fields are available. Both the historical and SSP585 (see Text S3 and Figure S3) experiments include a 92-member ensemble based on perturbed initial conditions (Table S1). For each model, we interpolated the raw U250 field into a commonly used spatial resolution of 2.5° × 2.5°. The historical

10.1029/2021GL093722

simulation for each model is individually classified following the same procedure on ERA5 for the historical period of 1979–2014. For each member, future daily U250 fields under the SSP585 experiment are assigned to classified types by matching the most similar type with the smallest Euclidean distance.

3. Results

3.1. $PM_{2.5}$ Pollution in Delhi

First, we revisited the particulate pollution of Delhi from January 2013 to February 2020. Figure 1a shows the annual mean concentrations of $PM_{2.5}$ over 2013–2019. Apparently, Delhi suffers from severe pollution, with annual mean $PM_{2.5}$ concentrations all exceeding 100 μg m^{-3} for 2013–2019. A statistically significant annual trend of −3.7 μg m^{-3} a^{-1} was observed, which manifested as more days under good and satisfactory air quality index (AQI) in 2019 than in 2013 (Figure 1d). No significant annual trends were identified for any of the four seasons, while seasonal mean $PM_{2.5}$ concentrations in the post-monsoon (October and November) and winter seasons (DJF, December-January-February) show interannual variations, which may be attributed to meteorological fluctuations. $PM_{2.5}$ in Delhi has a clear seasonality with a low concentration in the monsoon season (June-July-August-September) and high pollution during the post-monsoon and boreal winters (Figure 1c). Due to extensive biomass burning in Punjab, northwestern Delhi (Liu et al., 2018), $PM_{2.5}$ concentrations in the post-monsoon season have reached as high as 200 μg m^{-3}.

For winter, Delhi experienced no good AQI days (Figure 1e), and the very poor AQI days accounted for 55.8%–63.2% from 2013 to 2019. The mean $PM_{2.5}$ concentration during DJFs during 2013–2019 in Delhi was 192.4 μg m^{-3}, approximately five times the national $PM_{2.5}$ annual standard of India (40 μg m^{-3}). Severe polluted days with daily $PM_{2.5}$ exceeding 250 μg m^{-3} range between 21.9% and 31.1%, and such a high frequency of exposure under extreme polluted conditions would cause serious health impacts. Unlike post-monsoon emissions, emissions from local sources are reported to be more important in winter, contributing more than 70% of wintertime total $PM_{2.5}$ mass concentrations in Delhi (Guo et al., 2019). The frequent occurrence of severe pollution in Delhi is attributed to these high emissions coinciding with unfavorable weather conditions.

3.2. $PM_{2.5}$ Pollution Under Different Circulation Patterns

Four types of circulation patterns (Figure S4) of U250 (hereafter referred to as T1 through T4) are identified during boreal winter in the period of 1979–2019 (41 years; 3,760 days). T1-4 accounted for 27.1%, 18.2%, 26.9%, and 27.8% of the 3,760 days, respectively. Considering the average $PM_{2.5}$ concentrations and the average of the anomalies between daily $PM_{2.5}$ concentrations and 7-winter mean $PM_{2.5}$ concentrations to distinguish clean-favorable and pollution-favorable circulation patterns (Figure 2), T2 (217.5

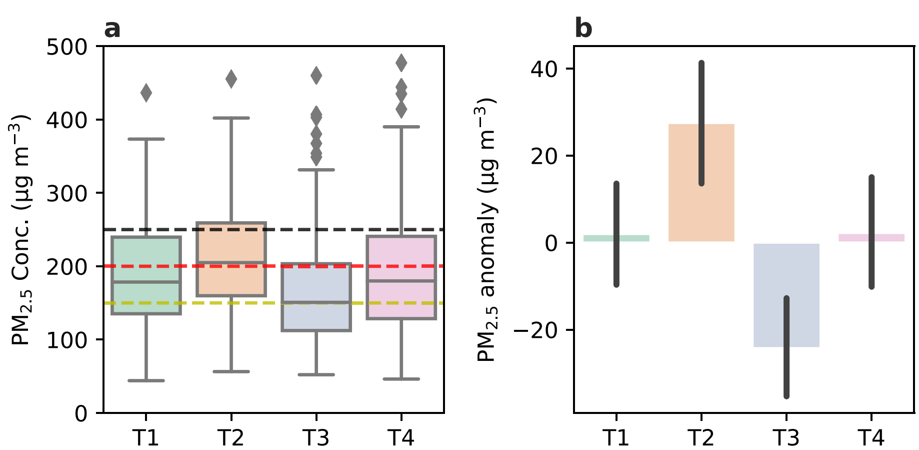

Figure 2. $PM_{2.5}$ pollutions under four circulation patterns. (a) Box plots of the daily average $PM_{2.5}$ concentrations under each circulation type. (b) Mean anomalies of $PM_{2.5}$ relative to the December-January-February means of 2013–2020 for each circulation type, and the error bars are computed based on a normal distribution 95% confidence interval. T2 (T3) is identified as a pollution- (clean-) favorable type because of its high positive (negative) $PM_{2.5}$ anomaly.

and +27.5 μg m^{-3}) is the severe pollution-favorable circulation type. More than 50% and 25% of days in T2 experience daily $PM_{2.5}$ above 200 μg m^{-3} and 250 μg m^{-3}, respectively. T1 (192.0 and +2.0 μg m^{-3}) and T4 (192.3 and +2.2 μg m^{-3}) are moderate pollution-favorable circulation patterns. Because winter $PM_{2.5}$ levels in Delhi were mostly at high levels (daily $PM_{2.5}$ concentration for about 90% days were above 100 μg m^{-3}), T3 (165.8 and −24.3 μg m^{-3}) is considered as relatively clean-favorable pattern with less occurrences of severe pollution. Such serious situation indicate that urgent actions are needed to reduce emissions. As for severe pollution events, there were more than 20.6% days with daily $PM_{2.5}$ exceeding 250 μg m^{-3} during DJFs over 2013–2019. Under such heavily polluted conditions, even cutting 50% of traffic emissions did not help (Chowdhury et al., 2017), which emphasizes the dominant role of meteorology during severe pollution.

Figure 3 shows the composite anomalies in weather conditions under each circulation pattern. The severe pollution-favorable circulation pattern T2 shows significant differences from the other circulation patterns. At 250 hPa, zonal winds present a dipole pattern with positive anomalies to the north and negative anomalies to the south of Delhi for T2 (Figure 3b). Accompanied by positive anomalies at a geopotential height of 500 hPa (Figure 3f), the upper-level circulation reveals a northward shift in the subtropical jet stream associated with the northward intrusion of the subtropical high, leading to fewer passes of cyclone systems and more dominance of the subtropical high (Figure 3j). As a result, anomalous downdrafts are found from the upper level (250 hPa) to the near surface (850 hPa), indicating stagnant conditions over IGP (Figure 3n). The strengthened downdrafts would induce a warm and dry layer above the planetary boundary layer (PBL) (Figure 3n), which restricted the vertical diffusion of pollutants. As $PM_{2.5}$ accumulates, more solar radiation scatters back to space, reducing the near-surface temperature and enhancing the relative humidity

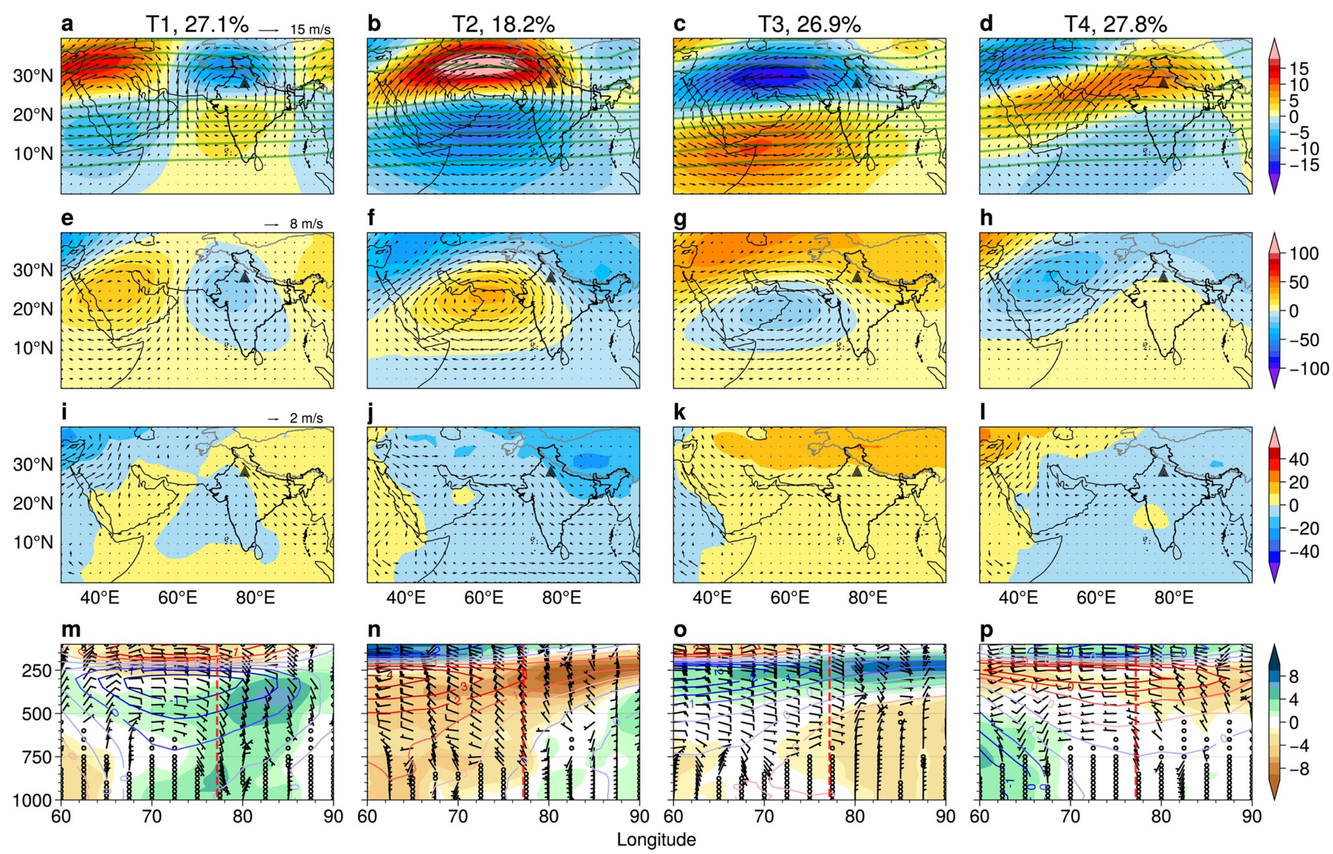

Figure 3. Weather conditions under each circulation type. (a–l) Composited anomalous weather patterns of (a–d) U250 (m s^{-1}, shading) and 250 hPa winds (m s^{-1}, vector), (e–h) geopotential height (m, shading) and winds (m s^{-1}, vector) at 500 hPa, (i–l) geopotential height (m, shading) and winds (m s^{-1}, vector) at 850 hPa, and (m–p) pressure-longitude cross sections of the relative humidity (%, shading) and temperature (°C, contour) for T1 to T4 over the years 2013–2019. The cross sections in (m–p) are averaged over 27.5–30°N. The inset text in (a–d) shows the frequency of occurrences for each type during December-January-February (DJF) in 1979–2019. The gray contours in (a–d) are the subtropical jet streams calculated by DJF means of U250 from 1981 to 2010.

(Figure 3n). Such meteorological conditions further increase near-surface $PM_{2.5}$ concentrations through complex chemical reactions.

In contrast, clean-favorable circulation T3 displayed the opposite pattern of U250 compared with T2 (Figures 3c–3k and 3o). Cyclone anomalies are identified for T3 and are associated with WDs, which originate in the Mediterranean region and are embedded in the subtropical westerly jet stream. When the subtropical westerly jet shifts southward (Figure 3c), WDs pass through the IGP, corresponding to circulation pattern T3. Then, strong winds, high PBL heights and enhanced wet depositions due to convective weather conditions (ascending airflows over the IGP) are favorable for the dispersion of pollutants (Figures 3k and 3o).

Both T1 and T3 are associated with WDs, which bring precipitation to mitigate ambient $PM_{2.5}$ through wet deposition (Figure S5). The precipitation in T1 covers most of India, and such cloudy weather restricts the evolution of the PBL (Figure S6a). The anomalous eastern winds at 850 hPa (Figure 3i) weaken the horizontal dispersion of pollutants in Delhi. All these conditions lead to higher $PM_{2.5}$ concentrations under T1 circulation than under T3 circulation. In contrast, T2 and T4 are under the control of an anticyclonic system associated with descending motions in Delhi. T2 has the lowest PBL (Figure S6b), and the entire IGP is dominated by northwestern flows. We notice there are high AOD loadings in the northwest of Delhi (Figure S7b), which may enhance $PM_{2.5}$ concentrations in Delhi under the influence of northwestern airflows (Figure 3j). A previous study also found more regional transport of pollutants to Delhi during highly polluted episodes (Guo et al., 2019). Therefore, $PM_{2.5}$ concentration under T2 circulation is higher than it is under T3 circulation.

Historical long-term variations in the wintertime frequencies of each circulation pattern for 1979–2019 were also investigated (Figure S8). The frequencies of the four circulation patterns have no significant trends in winter over 1979–2019, but strong interannual variations are observed. Observational evidence also showed that there was no significant trend in the WD frequency or the position of the subtropical westerly jet stream in the past 50 years (Hunt et al., 2019), which resembled our findings.

3.3. Future Projection

We evaluate the role of climate change by comparing the frequency of the winter circulation patterns between the historical period (1981–2010) and the future period (2020–2100) under the SSP585 scenario in 30 CMIP6 models. First, the performance of simulated historical circulations is evaluated by comparison with the classified circulation from the ERA5 data set. For each CMIP6 model member, the daily U250 in historical experiments is classified over 1979–2014. We found the simulated historical circulation patterns compared well with the observed spatial distribution, with most models showing spatial correlation higher than 0.9, and the standard deviation ratios ranged between 0.9 and 1.2 (Figure S9). Then the daily U250 under the SSP585 scenario over 2020–2100 is assigned to its most similar historical classification.

Under climate change, the frequencies of T1, T2, and T4 exhibit monotonic decreasing trends during the whole 21st century (Figures 4a, 4b and 4d). Our result is consistent with a previous study (Wu et al., 2019), which established a haze weather index and projected that meteorological conditions would be more beneficial for pollution dispersion during 2046–2054. For the severe pollution-favorable type T2, although the uncertainties of future projections rise from 2000 to 2100, more than 60% of ensemble members projected a reduced frequency of occurrence. In contrast, the frequency of the clean-favorable circulation pattern (T3) increases robustly (Figure 4c), which is supported by an intermember consensus, with more than 75% of ensemble members producing an increased frequency on clean-favorable days since 2020. Although the robustness of the future changes in pollution-favorable days and clean-favorable days in Deli, the 92 CMIP6 members still show slight disagreement in future projections under global warming scenarios, which mostly result from the uncertainty in the sensitivity of model physics and thermodynamics to global warming (Knutti & Sedláček, 2013). Compared with the 1981–2010 mean levels, the CMIP6 models project Delhi would experience two fewer days of severe pollution-favorable circulation pattern (T2) and seven more days of clean-favorable circulation pattern (T3) in 2070–2099. From 2020 to 2099, the linear trends for T2 and T3 are −0.34 and 1.06 days per decade (Figure S10), both are significant at 99% confident level. We also investigated future changes in the four circulation patterns under SSP126 and SSP370 scenario (see details in Text S4 and Figures S11–S14), which exhibit similar variations in four circulation patterns under SSP585

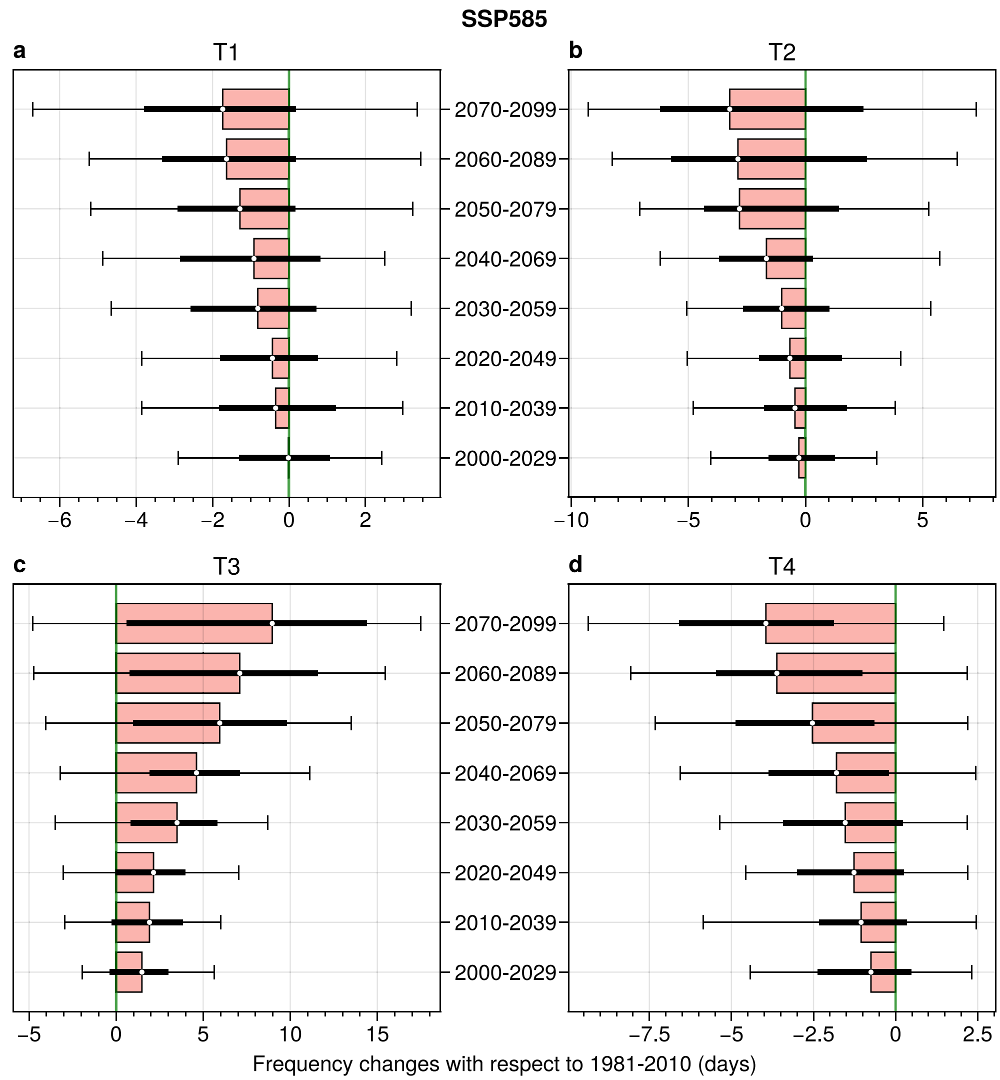

Figure 4. Future changes in the frequencies of four circulation types under SSP585 scenario based on 92 Coupled Model Intercomparison Project6 members. For each model member, the future changes in the mean frequencies of each circulation type are differences between future periods and historical period of 1981–2010. The whole error bar bounds are determined by 5% and 95% percentile values, and the central bold black lines denote interquartile range (25%–75%).

but with smaller linear trends. Besides meteorological conditions, anthropogenic emission is another factor inducing $PM_{2.5}$ pollutions. Since the SSP585 is a "fossil-fueled development" scenario, SO_2 and NOx emissions (mainly from energy, industrial and transportation) peak until 2040 (Figure S15). Therefore, although meteorological conditions are projected to mitigate $PM_{2.5}$ pollutions in Delhi since 2020, the high anthropogenic emissions may increase the risk of severe pollution before 2040.

What is responsible for the opposite changes between pollution- and clean-favorable weather conditions under global warming? Previous studies indicated that the sea surface temperature (SST) greatly impacts the winter circulation in India (Abid et al., 2021; Schott et al., 2009; Yadav et al., 2009). Moreover, aerosol pollution in northern India has been linked to sea surface temperature anomalies in the Pacific and Indian Oceans (Gao et al., 2019). To explore the underlying climate factors that are responsible for the polluted circulation pattern, we conduct correlation analyses to find signals from sea surface temperature. Figure S16 shows the correlation coefficient between SST and T2, which presented an ENSO Modoki-like SST anomaly pattern from 1979 to 2019, with a significant negative correlation identified in the center of the Pacific Ocean. The historical frequency of T2 has a close relation with the ENSO Modoki index (EMI;

download from http://www.jamstec.go.jp/frsgc/research/d1/iod/modoki_home.html.en), with a statistically significant correlation coefficient of −0.5, which passes the 99% confidence level. Significant negative correlations also exist in the North Atlantic Ocean. The SST index in the North Atlantic Ocean (SST-Atl), defined as SST anomalies averaged in the area of 80°–20°W, 5°–25°N, also has a negative correlation with the historical frequency of T2 with a correlation coefficient of −0.5. The SST-Atl and EWI have no significant relationship. During La Niña Modoki events (EMI < −0.5), significant negative anomalies expanding from the Arabian Peninsula to the Bay of Bengal and positive anomalies over northern India and Iran are induced (Graf & Zanchettin, 2012; He et al., 2021), implying a northward subtropical jet stream similar to T2 (Figure S17a). Additionally, the decline in North Atlantic SST over 80°–20°W, 5°–25°N (SST-Atl < 0) leads to an atmospheric wave train that excites a northward subtropical jet stream over India (Chen et al., 2019; Watanabe, 2004) (Figure S17b). Opposite SST forcing may induce clean-favorable conditions (T3).

During the historical period of 1979–2019, the combined opposite effect of the La Niña-like trend in Pacific SST and the warming trend in North Atlantic SST on weather conditions over India (Figure S18) might be responsible for the insignificant trends in T2 and T3 (Figure S8). However, for future scenario under SSP585, an El Niño-like trend occurs in the tropical Pacific Ocean, and a warming trend is located in the North Atlantic Ocean under climate change (Figures S19 and S20). These two factors conspire to generate an increasing frequency of clean-favorable circulation pattern and a decreasing frequency of severe pollution-favorable circulation pattern.

4. Conclusion

This study investigated the meteorological mechanisms in the formation of wintertime $PM_{2.5}$ pollution in Delhi, and future frequency changes in four circulation patterns were also projected under a warming scenario of SSP585. The annual mean $PM_{2.5}$ concentrations in Delhi all exceeded 100 $\mu g\ m^{-3}$ during 2013–2019. Although a statistically significant annual trend of −3.7 $\mu g\ m^{-3}\ a^{-1}$ was observed, no significant annual trends were identified for the four seasons. Based on the SOM classification technique, four typical weather patterns are identified in winters for 2013–2019 in Delhi. The severe pollution-favorable circulation pattern is characterized by a northward shift in subtropical jet streams, accompanied by a northward intrusion of the subtropical high, leading to descending anomalies from the upper troposphere to the near surface. Combined, the resultant lower passage of WDs, lower PBL, weakened winds and less precipitation contributed to severe particulate pollution in Delhi in wintertime. Under the future SSP585 scenario, Delhi is projected to experience two fewer days of severe pollution-favorable circulation pattern and seven more days of clean-favorable circulation pattern. We further explored the potential underlying cause and found that the time series of wintertime frequency of the severe pollution-favorable circulation pattern T2 was correlated with the cooling SST anomaly pattern in the central Pacific and North Atlantic Ocean over 1979–2019. However, CMIP6 models under SSP585 scenarios during future periods of 2020–2099 display warming trends in these two areas, leading to fewer occurrences of severe pollution-favorable days. We conclude that future meteorological conditions would be beneficial for air pollution improvement in India under climate change.

Data Availability Statement

The $PM_{2.5}$ observation is obtained from the https://in.usembassy.gov/embassy-consulates/new-delhi/air-quality-data/and https://www.airnow.gov/international/us-embassies-and-consulates/#India$New_Delhi. The ERA5 reanalysis data are available from https://cds.climate.copernicus.eu/cdsapp#!/dataset/reanalysis-era5-pressure-levels?tab=form. Aerosol optical depth (AOD) from Moderate Resolution Imaging Spectroradiometer (MODIS) aerosol products are obtained from https://ladsweb.modaps.eosdis.nasa.gov/search/. The daily global precipitation data are downloaded from https://psl.noaa.gov/data/gridded/data.cpc.globalprecip.html. CMIP6 outputs are available from https://esgf-node.llnl.gov/projects/cmip6/.

Acknowledgments
This work was supported by the National Natural Science Foundation of China (grant no. 42021004) and by the Major Research Plan of the National Social Science Foundation (grant no. 18ZDA052).

References

Abid, M. A., Kucharski, F., Molteni, F., Kang, I.-S., Tompkins, A. M., & Almazroui, M. (2021). Separating the Indian and Pacific Ocean impacts on the Euro-Atlantic response to ENSO and its transition from early to late winter. *Journal of Climate*, *34*(4), 1531–1548. https://doi.org/10.1175/jcli-d-20-0075.1

Callahan, C. W., & Mankin, J. S. (2020). The influence of internal climate variability on projections of synoptically driven Beijing haze. *Geophysical Research Letters*, *47*(11), e2020GL088548. https://doi.org/10.1029/2020gl088548

Chen, Y., Wild, O., Conibear, L., Ran, L., He, J., Wang, L., & Wang, Y. (2020). Local characteristics of and exposure to fine particulate matter ($PM_{2.5}$) in four Indian megacities. *Atmospheric Environment: X*, *5*, 100052. https://doi.org/10.1016/j.aeaoa.2019.100052

Chen, Z., Wu, R., & Wang, Z. (2019). Impacts of summer North Atlantic sea surface temperature anomalies on the East Asian winter monsoon variability. *Journal of Climate*, *32*(19), 6513–6532. https://doi.org/10.1175/jcli-d-19-0061.1

Chowdhury, S., & Dey, S. (2016). Cause-specific premature death from ambient $PM_{2.5}$ exposure in India: Estimate adjusted for baseline mortality. *Environment International*, *91*, 283–290. https://doi.org/10.1016/j.envint.2016.03.004

Chowdhury, S., Dey, S., Guttikunda, S., Pillarisetti, A., Smith, K. R., & Di Girolamo, L. (2019). Indian annual ambient air quality standard is achievable by completely mitigating emissions from household sources. *Proceedings of the National Academy of Sciences of the United States of America*, *116*(22), 10711–10716. https://doi.org/10.1073/pnas.1900888116

Chowdhury, S., Dey, S., Tripathi, S. N., Beig, G., Mishra, A. K., & Sharma, S. (2017). "Traffic intervention" policy fails to mitigate air pollution in megacity Delhi. *Environmental Science & Policy*, *74*, 8–13. https://doi.org/10.1016/j.envsci.2017.04.018

Cohen, A. J., Brauer, M., Burnett, R., Anderson, H. R., Frostad, J., Estep, K., et al. (2017). Estimates and 25-year trends of the global burden of disease attributable to ambient air pollution: An analysis of data from the Global Burden of Diseases Study 2015. *The Lancet*, *389*(10082), 1907–1918. https://doi.org/10.1016/S0140-6736(17)30505-6

David, L. M., Ravishankara, A. R., Kodros, J. K., Pierce, J. R., Venkataraman, C., & Sadavarte, P. (2019). Premature mortality due to $PM_{2.5}$ over India: Effect of atmospheric transport and anthropogenic emissions. *Geohealth*, *3*(1), 2–10. https://doi.org/10.1029/2018gh000169

Dey, S., Purohit, B., Balyan, P., Dixit, K., Bali, K., Kumar, A., et al. (2020). A satellite-based high-resolution (1-km) ambient $PM_{2.5}$ database for India over two decades (2000–2019): Applications for air quality management. *Remote Sensing*, *12*(23), 3872. https://doi.org/10.3390/rs12233872

Dimri, A. P., Yasunari, T., Kotlia, B. S., Mohanty, U. C., & Sikka, D. R. (2016). Indian winter monsoon: Present and past. *Earth-Science Reviews*, *163*, 297–322. https://doi.org/10.1016/j.earscirev.2016.10.008

Gao, M., Sherman, P., Song, S., Yu, Y., Wu, Z., & McElroy, M. B. (2019). Seasonal prediction of Indian wintertime aerosol pollution using the ocean memory effect. *Science Advances*, *5*(7), eaav4157. https://doi.org/10.1126/sciadv.aav4157

Graf, H.-F., & Zanchettin, D. (2012). Central Pacific El Niño, the "subtropical bridge," and Eurasian climate. *Journal of Geophysical Research*, *117*, 1102. https://doi.org/10.1029/2011jd016493

Gunthe, S. S., Liu, P., Panda, U., Raj, S. S., Sharma, A., Darbyshire, E., et al. (2021). Enhanced aerosol particle growth sustained by high continental chlorine emission in India. *Nature Geoscience*, *14*(2), 77–84. https://doi.org/10.1038/s41561-020-00677-x

Guo, H., Kota, S. H., Sahu, S. K., & Zhang, H. (2019). Contributions of local and regional sources to $PM_{2.5}$ and its health effects in north India. *Atmospheric Environment*, *214*, 116867. https://doi.org/10.1016/j.atmosenv.2019.116867

He, L., Hao, X., & Han, T. (2021). The asymmetric impacts of ENSO modoki on boreal winter climate over the Pacific and its rim. *Climate Dynamics*, *56*(1), 29–44. https://doi.org/10.1007/s00382-020-05395-z

Hersbach, H., Bell, B., Berrisford, P., Hirahara, S., Horányi, A., Muñoz-Sabater, J., et al. (2020). The ERA5 global reanalysis. *Quarterly Journal of the Royal Meteorological Society*, *146*(730), 1999–2049. https://doi.org/10.1002/qj.3803

Horton, D. E., Johnson, N. C., Singh, D., Swain, D. L., Rajaratnam, B., & Diffenbaugh, N. S. (2015). Contribution of changes in atmospheric circulation patterns to extreme temperature trends. *Nature*, *522*(7557), 465–469. https://doi.org/10.1038/nature14550

Horton, D. E., Skinner, C. B., Singh, D., & Diffenbaugh, N. S. (2014). Occurrence and persistence of future atmospheric stagnation events. *Nature Climate Change*, *4*, 698–703. https://doi.org/10.1038/nclimate2272

Hunt, K. M. R., Turner, A. G., & Shaffrey, L. C. (2018). The evolution, seasonality and impacts of western disturbances. *Quarterly Journal of the Royal Meteorological Society*, *144*(710), 278–290. https://doi.org/10.1002/qj.3200

Hunt, K. M. R., Turner, A. G., & Shaffrey, L. C. (2019). Representation of western disturbances in CMIP5 models. *Journal of Climate*, *32*(7), 1997–2011. https://doi.org/10.1175/jcli-d-18-0420.1

Knutti, R., & Sedláček, J. (2013). Robustness and uncertainties in the new CMIP5 climate model projections. *Nature Climate Change*, *3*(4), 369–373. https://doi.org/10.1038/nclimate1716

Kohonen, T., Schroeder, M. R., & Huang, T. S. (2001). *Self-organizing maps*. Springer-Verlag.

Li, J., Liao, H., Hu, J., & Li, N. (2019). Severe particulate pollution days in China during 2013–2018 and the associated typical weather patterns in Beijing-Tianjin-Hebei and the Yangtze River Delta regions. *Environmental Pollution*, *248*, 74–81. https://doi.org/10.1016/j.envpol.2019.01.124

Liao, Z., Sun, J., Yao, J., Liu, L., Li, H., Liu, J., et al. (2018). Self-organized classification of boundary layer meteorology and associated characteristics of air quality in Beijing. *Atmospheric Chemistry and Physics*, *18*(9), 6771–6783. https://doi.org/10.5194/acp-18-6771-2018

Liu, T., Marlier, M. E., DeFries, R. S., Westervelt, D. M., Xia, K. R., Fiore, A. M., et al. (2018). Seasonal impact of regional outdoor biomass burning on air pollution in three Indian cities: Delhi, Bengaluru, and Pune. *Atmospheric Environment*, *172*, 83–92. https://doi.org/10.1016/j.atmosenv.2017.10.024

Nair, V. S., Moorthy, K. K., Alappattu, D. P., Kunhikrishnan, P. K., George, S., Nair, P. R., et al. (2007). Wintertime aerosol characteristics over the Indo-Gangetic Plain (IGP): Impacts of local boundary layer processes and long-range transport. *Journal of Geophysical Research*, *112*(D13). https://doi.org/10.1029/2006jd008099

Ojha, N., Sharma, A., Kumar, M., Girach, I., Ansari, T. U., Sharma, S. K., et al. (2020). On the widespread enhancement in fine particulate matter across the Indo-Gangetic Plain toward winter. *Scientific Reports*, *10*(1), 5862. https://doi.org/10.1038/s41598-020-62710-8

Rayner, N. A., Parker, D. E., Horton, E. B., Folland, C. K., Alexander, L. V., Rowell, D. P., et al. (2003). Global analyses of sea surface temperature, sea ice, and night marine air temperature since the late nineteenth century. *Journal of Geophysical Research*, *108*, 4407. https://doi.org/10.1029/2002jd002670

Schnell, J. L., Naik, V., Horowitz, L. W., Paulot, F., Mao, J., Ginoux, P., et al. (2018). Exploring the relationship between surface $PM_{2.5}$ and meteorology in Northern India. *Atmospheric Chemistry and Physics*, *18*(14), 10157–10175. https://doi.org/10.5194/acp-18-10157-2018

Schott, F. A., Xie, S.-P., & McCreary, Jr, J. P. (2009). Indian Ocean circulation and climate variability. *Reviews of Geophysics*, *47*(1). https://doi.org/10.1029/2007rg000245

Singh, V., Singh, S., & Biswal, A. (2020). Exceedances and trends of particulate matter ($PM_{2.5}$) in five Indian megacities. *The Science of the Total Environment*, *750*, 141461.

Sreekanth, V., Mahesh, B., & Niranjan, K. (2018). Gradients in $PM_{2.5}$ over India: Five city study. *Urban Climate*, *25*, 99–108. https://doi.org/10.1016/j.uclim.2018.06.001

Venkataraman, C., Brauer, M., Tibrewal, K., Sadavarte, P., Ma, Q., Cohen, A., et al. (2018). Source influence on emission pathways and ambient $PM_{2.5}$ pollution over India (2015–2050). *Atmospheric Chemistry and Physics*, *18*(11), 8017–8039. https://doi.org/10.5194/acp-18-8017-2018

Watanabe, M. (2004). Asian jet waveguide and a downstream extension of the North Atlantic oscillation. *Journal of Climate*, *17*(24), 4674–4691. https://doi.org/10.1175/jcli-3228.1

Wu, X., Xu, Y., Kumar, R., & Barth, M. (2019). Separating emission and meteorological drivers of mid-21st-century air quality changes in India based on multiyear global-regional chemistry-climate simulations. *Journal of Geophysical Research: Atmospheres*, *124*(23), 13420–13438. https://doi.org/10.1029/2019jd030988

Yadav, R. K., Rupa Kumar, K., & Rajeevan, M. (2009). Increasing influence of ENSO and decreasing influence of AO/NAO in the recent decades over northwest India winter precipitation. *Journal of Geophysical Research*, *114*(D12). https://doi.org/10.1029/2008jd011318

Zhuang, Y., Fu, R., & Wang, H. (2020). Large-scale atmospheric circulation patterns associated with U.S. great plains warm season droughts revealed by self-organizing maps. *Journal of Geophysical Research: Atmospheres*, *125*(5), e2019JD031460. https://doi.org/10.1029/2019jd031460